Received: 25 June 2021 | Accepted: 20 September 2021

DOI: 10.1002/pamm.202100223

Greedy algorithms for image approximation from scattered Radon data

Kristof Albrecht[1,*] and **Armin Iske**[2,**]

[1] Technische Universität Hamburg, Institute of Mathematics, Am Schwarzenberg-Campus 3, D-21073 Hamburg
[2] Universität Hamburg, Department of Mathematics, Bundesstrasse 55, D-20146 Hamburg

Positive definite kernels are powerful tools for multivariate approximation from scattered data. This contribution discusses kernel-based image approximation from scattered Radon data. To this end, we use weighted kernels for the reconstruction. Moreover, we propose greedy algorithms, which are used to adaptively select suitable approximation spaces. This reduces the complexity of the resulting image reconstruction method and, moreover, it improves the numerical stability quite significantly.

1 Introduction

Computerized tomography (CT) requires reconstruction of an *attenuation function* $f : \mathbb{R}^2 \longrightarrow \mathbb{R}$ from line integrals

$$\mathcal{R}f(t,\theta) := \int_{\ell_{t,\theta}} f(x,y)\,dx\,dy = \int_{\mathbb{R}} f(t\cos(\theta) - s\sin(\theta), t\sin(\theta) + s\cos(\theta))\,ds, \tag{1}$$

where $\ell_{t,\theta} \subset \mathbb{R}^2$, for $(t,\theta) \in \mathbb{R} \times [0,\pi)$, denotes the unique straight line which passes through $(t\cos(\theta), t\sin(\theta))$ and is perpendicular to the unit vector $(\cos(\theta), \sin(\theta))$. The *Radon transform* $\mathcal{R} : L^1(\mathbb{R}^2) \longrightarrow L^1(\mathbb{R} \times [0,\pi))$ in (1) maps a bivariate function $f \equiv f(x,y)$ in Cartesian coordinates (x,y) to a bivariate function $\mathcal{R}f(t,\theta)$ in polar coordinates (t,θ).

The inversion of the Radon transform is given by the *filtered back projection (FBP) formula* [1]. The FBP formula, however, is highly sensitive to noise, where stabilization by low-pass filters diminish the shortcomings of FBP. Moreover, the application of the FBP formula relies on *regular* data, e.g. *parallel beam geometry*, which further limits the applicability of FBP in CT.

More flexible reconstructions are kernel-based scattered data approximation schemes. Just recently in [2], kernel-based approximation was adapted to the specific requirements of functional approximation from bivariate scattered Radon data. The method in [2] works with *weighted* kernels for the well-posedness of the reconstruction problem. Following along the lines of [2], we use greedy algorithms to select suitable approximation spaces. This leads to significant improvements on both the efficiency and the numerical stability of the kernel-based reconstruction.

2 Kernel-based reconstruction from scattered Radon data

To briefly explain the problem of kernel-based scattered Radon data reconstruction, let $\mathcal{L} = \{\ell_{t_j,\theta_j}\}_{j=1}^N \subset \mathbb{R}^2$ be a fixed set of N pairwise distinct straight lines in the plane. Any $f \in L^1(\mathbb{R}^2)$ gives a data vector $\mathcal{R}_\mathcal{L}(f) = ((\mathcal{R}f)(t_j,\theta_j))_{j=1}^N \in \mathbb{R}^N$ containing N scattered Radon samples from f, where from now we let $\mathcal{R}_j(f) := (\mathcal{R}f)(t_j,\theta_j)$, for $j = 1,\ldots,N$. Now, kernel-based reconstruction of f from $\mathcal{R}_\mathcal{L}(f)$ requires finding a solution to the interpolation problem $\mathcal{R}_\mathcal{L}(f) = \mathcal{R}_\mathcal{L}(s)$ by an interpolant $s : \mathbb{R}^2 \longrightarrow \mathbb{R}$ of the form

$$s(x) = \sum_{j=1}^N c_j \mathcal{R}_j^y K(x,y) \qquad \text{for } x \in \mathbb{R}^2, \tag{2}$$

where $\mathcal{R}_j^y$ denotes action of the Radon transform $\mathcal{R}_j$ on variable y and where $K \equiv K(x,y)$ is a positive definite kernel, i.e.,

$$A_{\mathcal{L},K} := \left(\mathcal{R}_j^x \mathcal{R}_k^y K(x,y)\right)_{1\le j,k\le N} \in \mathbb{R}^{N\times N}$$

is a symmetric positve definite matrix for any choice of finitely many pairwise distinct Radon lines $\mathcal{L}$. Therefore, the coefficients $c = (c_1,\ldots,c_N) \in \mathbb{R}^N$ of s in (2) are uniquely determined by the interpolation conditions $\mathcal{R}_\mathcal{L}(f) = \mathcal{R}_\mathcal{L}(s)$. Moreover, according to [2], the matrix entries in $A_{\mathcal{L},K}$ are well-defined for *weighted* kernels $K_w : \mathbb{R}^2 \times \mathbb{R}^2 \longrightarrow \mathbb{R}$ of the form

$$K_{\phi,w}(x,y) = \phi(\|x-y\|^2) w(\|x\|^2) w(\|y\|^2) \qquad \text{for } x,y \in \mathbb{R}^2,$$

where $\phi \equiv \phi(\|\cdot\|) \in L^1(\mathbb{R}^2) \cap \mathscr{C}(\mathbb{R}^2)$ is a positive definite kernel that is radially symmetric with respect to the Euclidean norm $\|\cdot\|$ on $\mathbb{R}^2$ and where $w \in L^1(\mathbb{R}^2) \cap \mathscr{C}(\mathbb{R}^2)$ is a positive *weight function*.

* kristof.albrecht@tuhh.de
** armin.iske@uni-hamburg.de

3 Greedy algorithms for data reduction

To reduce the complexity of the interpolation problem $\mathcal{R}_{\mathcal{L}}(f) = \mathcal{R}_{\mathcal{L}}(s)$, we determine a suitable *small* subset $\mathcal{S} \subset \mathcal{L}$ of *significant* Radon lines of size $n = |\mathcal{S}| \ll |\mathcal{L}| = N$. Then, the solution to the reconstruction problem boils down to solving the reduced interpolation problem on the Radon lines in $\mathcal{S}$. Hence, with the selection of the subset $\mathcal{S} \subset \mathcal{L}$, the linear approximation space $\mathcal{A}_{\mathcal{S}} := \text{span}\{(\mathcal{R}(t,\theta))^y K(\cdot, y) : \ell_{t,\theta} \in \mathcal{S}\}$ has *small* dimension $n \ll N$.

However, the selection of the subset $\mathcal{S} \subset \mathcal{L}$, and so the selection of the corresponding approximation space $\mathcal{A}_{\mathcal{S}} \subset \mathcal{A}_{\mathcal{L}}$ requires particular care. This is mainly for the sake of numerical stability, which may be critical in situations where two Radon lines in $\mathcal{S}$ are *close*, where two Radon lines $\ell_{t,\theta}$ and $\ell_{\tilde{t},\tilde{\theta}}$ are said to be *close*, iff their (unique) parameter points $(t,\theta), (\tilde{t},\tilde{\theta}) \in \mathbb{R} \times [0,\pi)$ are close with respect to the Euclidean norm on $\mathbb{R}^2$. This yields a metric on the set of planar Radon lines, whereby we can apply *greedy* data reduction. Adaptive thinning [3, 4] is only one example for a greedy data reduction scheme, which works with recursive point removals. We apply adaptive insertion of Radon lines from $\mathcal{L}$ by adaptive insertion of points from the *large* set $\mathcal{P}_{\mathcal{L}} = \{(t_j, \theta_j)\}_{j=1}^N$ of parameters that are defining $\mathcal{L}$.

We remark that related greedy methods were published in [5], where the terms P-*greedy* and h-*greedy* for two variants of greedy data reduction schemes were coined (for details we refer to [5]). This has led us to include two greedy algorithms: Each insertion of the *next* parameter point $(t_+, \theta_+) \in \mathbb{R} \times [0,\pi)$, from a current set of Radon parameter points $\mathcal{P}_{\mathcal{S}} \subset \mathcal{P}_{\mathcal{L}}$, is characterized by

$$(t_+, \theta_+) = \operatorname*{argmax}_{(t,\theta) \in \mathcal{P}_{\mathcal{L}} \setminus \mathcal{P}_{\mathcal{S}}} \min_{(s,\sigma) \in \mathcal{P}_{\mathcal{S}}} \|(t,\theta) - (s,\sigma)\| \qquad (h\text{-greedy}),$$

whereas each insertion of the *next* Radon functional $\mathcal{R}_+ \equiv \mathcal{R}(t_+, \theta_+)$ is characterized by

$$\mathcal{R}_+ = \operatorname*{argmax}_{(t,\theta) \in \mathcal{P}_{\mathcal{L}} \setminus \mathcal{P}_{\mathcal{S}}} \min_{\mu \in \mathcal{A}_{\mathcal{S}}} \|(\mathcal{R}(t,\theta))^y K(\cdot, y) - \mu\|_K \qquad (P\text{-greedy}),$$

where $\|\cdot\|_K$ denotes the *native* norm of the reproducing kernel Hilbert space (RKHS) generated by K.

4 Numerical example

We have performed numerical experiments, where we used the weighted kernel function

$$K_w(x,y) = e^{-3/2\|x\|_2^2} \cdot e^{-2000\|x-y\|_2^2} \cdot e^{-3/2\|y\|_2^2} \qquad \text{for } x, y \in \mathbb{R}^2.$$

We generated $N = 15,000$ Radon lines to reconstruct the bull's eye phantom. From each of the two greedy removal schemes we obtained a subset of $n = 5,000$ significant Radon lines. For comparison, we also included a set of n random Radon lines.

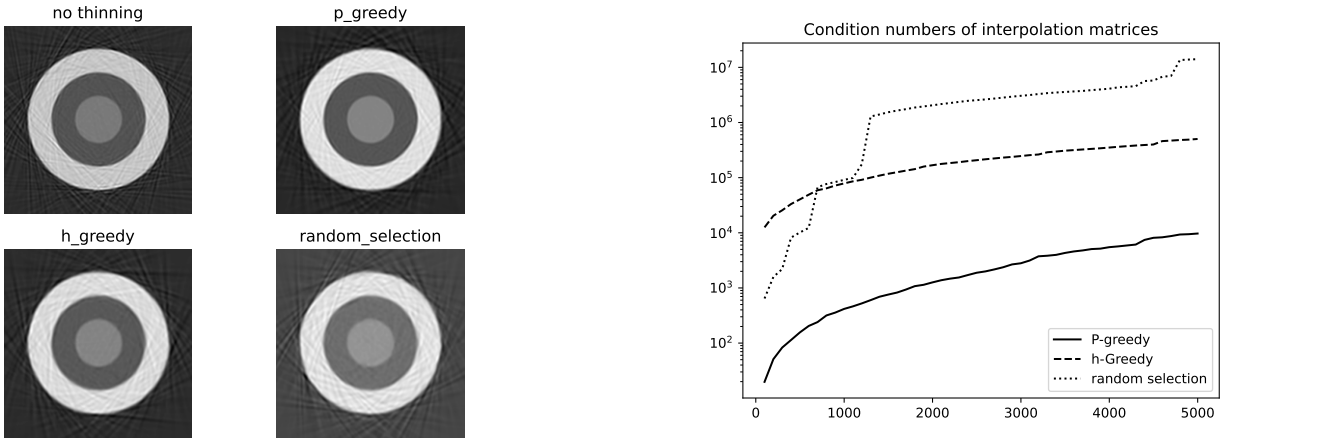

Fig. 1: Reconstruction of bull's eye with different algorithms (left); spectral condition numbers cond$(A_{\mathcal{S},K})$ as a function of $n = |\mathcal{S}|$ (right)

Acknowledgements The authors acknowledge the support by the Deutsche Forschungsgemeinschaft (DFG) within the Research Training Group GRK 2583 "Modeling, Simulation and Optimization of Fluid Dynamic Applications". Open access funding enabled and organized by Projekt DEAL.

References

[1] T. Feeman, The Mathematics of Medical Imaging, Springer Undergraduate Texts in Mathematics and Technology (Springer, 2015).

[2] S. DeMarchi, A. Iske, and G. Santin, Calcolo **55** (2018).
[3] L. Demaret, N. Dyn, and A. Iske, Signal Processing **86**, 1604–1616 (2006).
[4] N. Dyn, M. Floater, and A. Iske, Journal of Computational and Applied Mathematics **145**, 505–517 (2002).
[5] S. DeMarchi, R. Schaback, and H. Wendland, Adv. Comput. Math. **23**, 317–330 (2005).